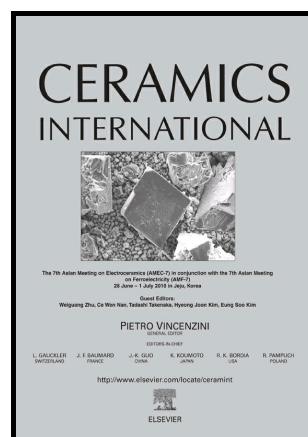


Author's Accepted Manuscript

Ag@CoFe₂O₄/Fe₂O₃ nanorod arrays on carbon fiber cloth as SERS substrate and photo-Fenton catalyst for detection and degradation of R6G

Lingling Bian, Yuanjun Liu, Guoxing Zhu, Chao Yan, Junhao Zhang, Aihua Yuan



www.elsevier.com/locate/ceri

PII: S0272-8842(18)30186-X
DOI: <https://doi.org/10.1016/j.ceramint.2018.01.172>
Reference: CERI17304

To appear in: *Ceramics International*

Received date: 3 December 2017
Revised date: 18 January 2018
Accepted date: 20 January 2018

Cite this article as: Lingling Bian, Yuanjun Liu, Guoxing Zhu, Chao Yan, Junhao Zhang and Aihua Yuan, Ag@CoFe₂O₄/Fe₂O₃ nanorod arrays on carbon fiber cloth as SERS substrate and photo-Fenton catalyst for detection and degradation of R6G, *Ceramics International*, <https://doi.org/10.1016/j.ceramint.2018.01.172>

This is a PDF file of an unedited manuscript that has been accepted for publication. As a service to our customers we are providing this early version of the manuscript. The manuscript will undergo copyediting, typesetting, and review of the resulting galley proof before it is published in its final citable form. Please note that during the production process errors may be discovered which could affect the content, and all legal disclaimers that apply to the journal pertain.

**Ag@CoFe₂O₄/Fe₂O₃ nanorod arrays on carbon fiber cloth as SERS
substrate and photo-Fenton catalyst for detection and degradation of
R6G**

Lingling Bian^a, Yuanjun Liu^{a,*}, Guoxing Zhu^c, Chao Yan^b, Junhao Zhang^a, Aihua Yuan^a

^a*School of Environmental and Chemical Engineering, Jiangsu University of Science and Technology, Zhenjiang, 212018, China.*

^b*School of Materials Science and Engineering, Jiangsu University of Science and Technology, Zhenjiang, 212003, China.*

^c*School of Chemistry and Chemical Engineering, Jiangsu University, Zhenjiang, 212013, China*

liuyuanjun@just.edu.cn;

aihua.yuan@just.edu.cn;

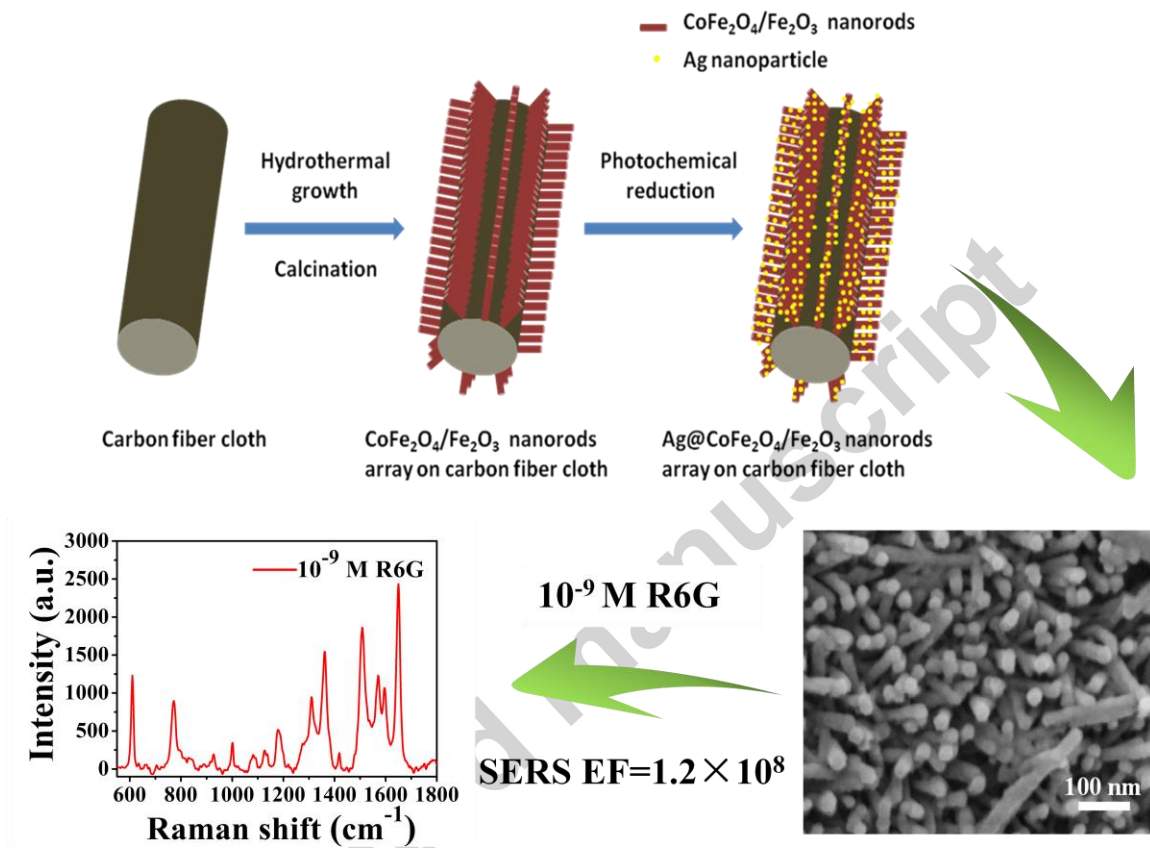
**fax: +86-511-85635850; Tel: +86-511-85639001*

Abstract

In this study, Ag nanoparticles loaded CoFe₂O₄/Fe₂O₃ nanorod arrays on carbon fiber cloth have been successfully fabricated by a hydrothermal route followed by a calcination treatment and photochemical reduction process. The as-prepared composite has been characterized by X-ray diffraction (XRD), scanning electron microscope (SEM), transmission electron microscope (TEM) and X-ray photoelectron spectroscopy (XPS). The obtained Ag@CoFe₂O₄/Fe₂O₃ nanorod arrays show excellent SERS performance, which provides enhancement factors (EF) as high as about 1.2×10^8 for Rhodamine 6G (R6G). The SERS signals collected over a $20 \mu\text{m} \times 20 \mu\text{m}$ area show relative standard deviation lower than 12%, suggesting good SERS signal uniformity. In addition, the Ag@CoFe₂O₄/Fe₂O₃ nanorod arrays can be used as an effective photo-Fenton catalyst photocatalytic degradation of R6G. It was found that 99.15% of R6G can be degraded in an hour. This bifunctional composite that can act both as SERS substrates and as photo-Fenton catalyst would facilitate the cleaning and recycling of SERS substrates for reusing through a photocatalytic process, as well as facilitate the integration of rapid detection and effective degradation of organic pollutants.

Key words: Ag@CoFe₂O₄/Fe₂O₃ nanorod arrays, SERS, photo-Fenton catalyst, recyclable substrate, R6G

Graphical abstract:



1. Introduction

How to detect organic pollutants at ultralow concentration is always a hot research topic. Surface-enhanced Raman scattering (SERS) is a sensitive and nondestructive analytical detection tool and can detect analytes even to a single molecule [1-3]. Noble metal (such as Ag, Au) nanostructures have been widely investigated to be the SERS substrate owing to the enhanced electromagnetic near field on the surface of metal nanostructure aggregation, which can highly amplify the Raman signal [4-7]. However, fabrication of SERS substrates with large area, high sensitivity and excellent reproducibility still remains challenging. Two dimensional and three dimensional (2D and 3D) noble metal nanoparticle arrays such as Au nanocluster [8-9], Ag nanoparticles decorated 3D sunflower-like structure [10], Au coated ZnO [11-12], Ag coated TiO₂ [13-14], Ag coated NiO [15] were widely prepared and used as SERS substrates, most of which show excellent SERS signals with improved reproducibility[16-19].

In addition to the detection technology, remove of pollutants after detection is another very important issue. Photocatalytic degradation route is a rapid, cost effective and energy-saving method to remove of various dye pollutants [20-22]. Thus, systematic integration of rapid detection and effective degradation of organic pollutants has attracted more and more attention. Recently, it was reported that metal-semiconductor nanocomposites can act as photocatalysts to degrade dye pollutants. At the same time, they show excellent SERS performance. This makes them a kind of potential bifunctional materials as both of photocatalysts and SERS substrates that can detect and remove of pollutants at the same time. For examples, it was demonstrated that detection and visible-light photocatalytic degradation of Sudan 1 can be finished by Au nanoparticles decorated AgCl or AgBr micro-necklaces [23]. ZnO-RGO-Au composite was also employed both as a photocatalyst for degrading R6G and a SERS substrate for real-time quantitatively monitoring of the degradation process [24]. In addition, some TiO₂-noble metal nanocomposites and ZnO-noble metal nanocomposites were also prepared and used as SERS substrates and photocatalysts [25-28]. These pioneering studies suggest the wide application of SERS substrates composed by metal-semiconductor composites, which facilitate the integration of real-time detection and effective degradation. However,

the reported bifunctional metal-semiconductor substrates are limited to several cases. There is still a huge space for developing this kind of bifunctional SERS substrates. Herein, we demonstrate a new metal-semiconductor composite SERS substrate composed by Ag and CoFe₂O₄/Fe₂O₃ nanorod arrays.

It is known that ferrites are useful soft magnetic materials. They are also effectively heterogeneous photocatalysts, which can produce e⁻/h⁺ pairs on the surface under light irradiation [29]. The produced e⁻ and h⁺ enable oxidation and reduction processes to occur, which usually involve the formation of reactive oxygen species, such as highly active hydroxyl radicals (·OH). With the addition of H₂O₂, the production of ·OH can be enhanced and a Fenton-type system is generated. The obtained ·OH radicals can oxidize most of organic contaminants in waste water [30-34]. Thus, the integration of noble metal nanoparticles with ferrites will produce magnetic bifunctional SERS substrates with effectively photocatalytic performance.

The bifunctional composites, Ag@CoFe₂O₄/Fe₂O₃ nanorod arrays, were synthesized via hydrothermal method followed by a photochemical route. The obtained composite can act as both of photocatalysts and SERS substrates. It exhibits high SERS sensitivity and excellent reproducibility. The EF and detection limit can reach 1.2×10^8 and 10^{-10} M for R6G, respectively. It was found that the composite has enhanced SERS performance than those of CoFe₂O₄/Fe₂O₃ nanorod arrays and Ag nanoparticle substrate. The signals collected over a 20 μm×20 μm area of Ag@CoFe₂O₄/Fe₂O₃ nanorod arrays give relative standard deviation lower than 12%. In addition, the composite can serve as a photo-Fenton catalyst to degrade R6G effectively. The photodegradation results showed that with the assistance of Ag@CoFe₂O₄/Fe₂O₃ nanorod arrays, the degradation rate of the R6G solution (5mg/L) was 99.15% after 1 h, which is much higher than that of pristine CoFe₂O₄/Fe₂O₃ nanorod arrays. Especially, it was demonstrated that the bifunctional SERS substrate can be recycled with the assistance of a photocatalytic degradation process, which will help to clean the absorbed molecular on the surface.

2. Experimental details

2.1. Materials

Cobalt nitrate hexahydrate ($\text{Co}(\text{NO}_3)_2 \cdot 6\text{H}_2\text{O}$), ferric nitrate nonahydrate ($\text{Fe}(\text{NO}_3)_3 \cdot 9\text{H}_2\text{O}$), silver nitrate (AgNO_3), ammonium fluoride (NH_4F), nitric acid (HNO_3 , 68_{wt}%) and urea were purchased from Sinopharm Chemical Reagent Co, Ltd. R6G was purchased from J&K Scientific, Ltd. All the chemicals were of analytical grade and used without further purification. The carbon fiber cloth (WOS1002, purchased from CeTech Corporation, Taiwan) was cut into pieces with size of 2 cm \times 2 cm square shape, which was washed by ultrasonic treatment in acetone, distilled water and ethanol for one hour, respectively. Then it was soaked in the nitric acid solution (HNO_3 , 68_{wt}%) for 4 hours to activate the surface.

2.2. Synthesis of $\text{Ag}@\text{CoFe}_2\text{O}_4/\text{Fe}_2\text{O}_3$ nanorod arrays

The $\text{Ag}@\text{CoFe}_2\text{O}_4/\text{Fe}_2\text{O}_3$ nanorod arrays was synthesized via a three-step experimental process. Typically, 1 mmol of $\text{Co}(\text{NO}_3)_2 \cdot 6\text{H}_2\text{O}$, 2 mmol of $\text{Fe}(\text{NO}_3)_3 \cdot 9\text{H}_2\text{O}$, 2 mmol of NH_4F , and 5 mmol of urea were dissolved successively into 20 mL distilled water under continuous stirring for 30 min. Then the mixture was transferred into 25 mL Teflon-lined stainless-steel autoclave. A piece of treated carbon fiber cloth was placed in it. Afterwards, the autoclave was heated up to 140 °C and reacted at that temperature for 10 h. When cooled to room temperature naturally, the carbon fiber cloth was taken out and washed with distilled water for several times. It was calcined at 450 °C in N_2 atmosphere for 2 h. The obtained sample, $\text{CoFe}_2\text{O}_4/\text{Fe}_2\text{O}_3$ nanorod arrays on carbon fiber cloth, was then immersed in 0.5 mL of 0.05 M AgNO_3 aqueous solution and was irradiated by UV-light for 3h at room temperature. UV light irradiation induces the formation of Ag nanoparticles on $\text{CoFe}_2\text{O}_4/\text{Fe}_2\text{O}_3$ nanorod arrays, forming $\text{Ag}@\text{CoFe}_2\text{O}_4/\text{Fe}_2\text{O}_3$ nanorod arrays.

2.3 Characterization

The phase identification of the samples were characterized via powder X-ray diffraction (XRD, Shimadzu XRD-6000 diffractometer, Cu-K α radiation, $\lambda=0.15406$ nm). The morphologies and microstructures were observed via scanning electron microscopy (SEM, Hitachi S4800 microscope) and transmission electron microscopy (TEM, Tecnai G2 F30 S-Twin, FEI, Netherlands), respectively. The chemical composition was executed by X-ray photoelectron spectroscopy (XPS, Thermo-VG Scientific ESCALAB 250 using Al-K α radiation).

2.4 SERS measurements

Surface-enhanced Raman scattering analysis was conducted with a Raman spectrometer (Renishaw Via, England). All of the Raman measurements were performed at room temperature. For Raman scattering measurements, the synthesized SERS substrates and the pure carbon cloth substrate were soaked in 3 mL of R6G aqueous solutions with different concentrations for 12 h. Then, the substrates were taken out and dried in dark place. A 532 nm laser was used as the excitation source with an exposure time of 2 s and every resultant spectrum was accumulated two times. The laser power was maintained at 22.5 mW (0.05% \times 45 W) with an average spot size about 2 μ m diameter in all acquisitions. The identical instrumental settings were used for all the Raman tests.

2.5 Degradation of R6G dye

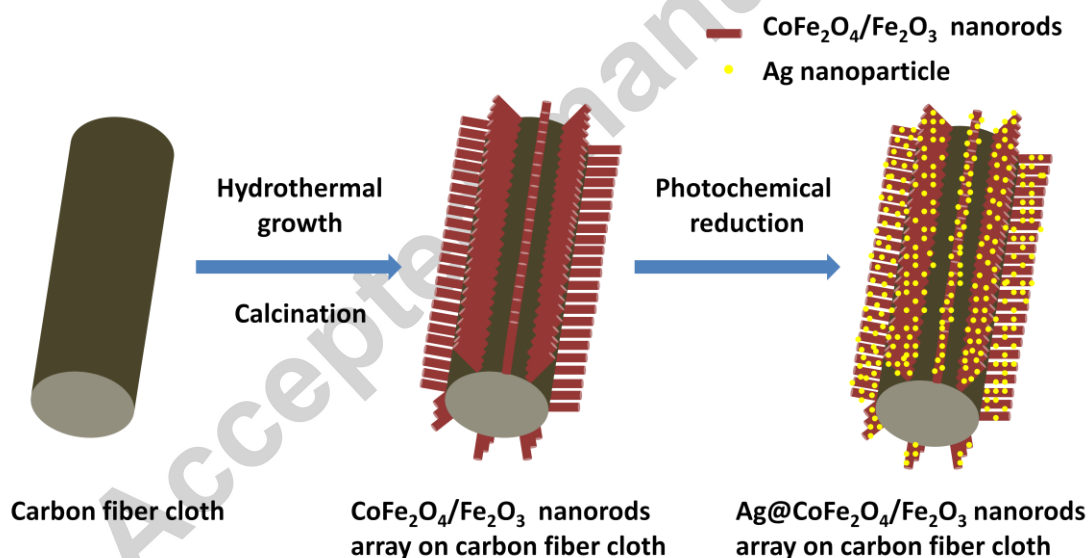
The photo-Fenton experiments were performed in a photochemical reaction apparatus (QIQIAN-V, Shanghai Qiqian Electronic technology Co. Ltd.). A 300 W Xe lamp with wavelength range of 300 to 800 nm was used to simulate sunlight. The concentration of R6G was analyzed by using a UV-vis spectrophotometer (UV-3010, Hitachi). The photocatalytic performance of the Ag@CoFe₂O₄/Fe₂O₃ nanorod arrays was evaluated by degradation of R6G in aqueous solution. All the experiments were performed at room temperature under ambient conditions. In a typical experiment, a piece of carbon fiber cloth with Ag@CoFe₂O₄/Fe₂O₃ nanorod arrays was immersed in 50 mL of R6G (5 mg/L) solution. The solution was then magnetically stirred in the dark for 30 min before light irradiation.

Then, 1 mL of 30% H_2O_2 was added. The concentration change of R6G was analyzed every 5 min with 2 mL aliquots taking from the reaction system by using UV-vis spectroscopy. For comparison, photocatalytic degradation of R6G on $\text{CoFe}_2\text{O}_4/\text{Fe}_2\text{O}_3$ nanorod arrays was also investigated.

2.6 The recycling of the $\text{Ag}@\text{CoFe}_2\text{O}_4/\text{Fe}_2\text{O}_3$ nanorod arrays SERS substrate

After the first time use, the $\text{Ag}@\text{CoFe}_2\text{O}_4/\text{Fe}_2\text{O}_3$ nanorod arrays were put into 20 mL of H_2O_2 solution (containing 0.8 mL of 30% H_2O_2) for 30 mins under Xe lamp. After washing with distilled water, the SERS substrate was soaking into 3 mL of 10^{-6} M R6G for 12 h again.

3. Results and discussion



Scheme 1. Schematic illustration for the fabrication of Ag nanoparticles decorated $\text{CoFe}_2\text{O}_4/\text{Fe}_2\text{O}_3$ nanorod arrays grafted on carbon fiber cloth.

$\text{Ag}@\text{CoFe}_2\text{O}_4/\text{Fe}_2\text{O}_3$ nanorod arrays on carbon fiber cloth were fabricated through a two-step experimental process. Scheme 1 illustrates the fabrication procedure. $\text{CoFe}_2\text{O}_4/\text{Fe}_2\text{O}_3$ nanorod arrays were firstly prepared by a hydrothermal growth route followed by a calcination treatment process. Due

to the presence of $\text{CoFe}_2\text{O}_4/\text{Fe}_2\text{O}_3$ nanorod arrays, the composite can be easily collected from the solution by a magnet. After that, the carbon fiber cloth loaded with $\text{CoFe}_2\text{O}_4/\text{Fe}_2\text{O}_3$ nanorod arrays was then immersed in AgNO_3 solution. Ag nanoparticles were generated on the surface of $\text{CoFe}_2\text{O}_4/\text{Fe}_2\text{O}_3$ nanorod arrays through an in situ photochemical reduction process.

Fig.1 shows the XRD pattern of the $\text{CoFe}_2\text{O}_4/\text{Fe}_2\text{O}_3$ nanorod arrays after calcination, the diffraction peaks at 18.3° , 30.1° , 35.4° , 37.1° , 43.1° , 53.4° , 56.9° and 62.6° can be indexed to (111), (220), (311), (222), (400), (422), (511) and (440) crystal planes of cubic phase CoFe_2O_4 (JCPDS No.22-1086), respectively. The diffraction peaks at 24.1° , 33.1° , 35.6° , 40.8° , 43.5° , 49.5° , 54.1° , and 57.6° can be well assigned to (012), (104), (110), (113), (202), (024), (116) and (018) crystal planes of Fe_2O_3 (JCPDS No.33-0664), respectively. Most of the diffraction peaks are intense and sharp, indicating that the as-prepared product possesses remarkable crystalline. Apparently, the broad peak at 26.36° can be well indexed to carbon fiber cloth. These results demonstrate crystalline $\text{CoFe}_2\text{O}_4/\text{Fe}_2\text{O}_3$ nanorod arrays have been integrated on to carbon fiber cloth.

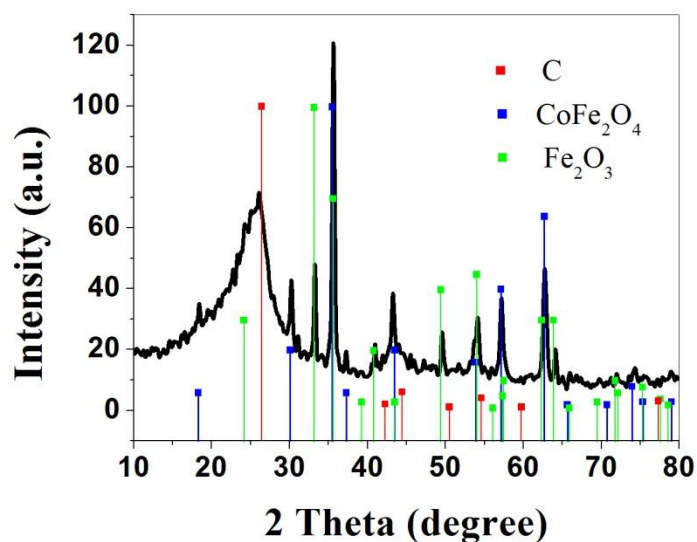


Fig. 1. XRD pattern of $\text{CoFe}_2\text{O}_4/\text{Fe}_2\text{O}_3$ nanorod arrays on carbon fiber cloth after calcination.

The morphology of the as-prepared $\text{CoFe}_2\text{O}_4/\text{Fe}_2\text{O}_3$ nanorod arrays product was observed by SEM and TEM. The SEM image of blank carbon fiber before loading materials is shown in Fig. 2(a), the diameter of the carbon fiber is around $10\ \mu\text{m}$ and the surface is smooth. After hydrothermal and calcination process, amounts of nanorods with diameter in range of $40\text{--}90\ \text{nm}$ appears on carbon fiber surface (Fig. 2(b-c)). Fig. 2(d) shows that the average diameter of $\text{CoFe}_2\text{O}_4/\text{Fe}_2\text{O}_3$ nanorods is about $70\ \text{nm}$. This is consistent with the SEM results. These $\text{CoFe}_2\text{O}_4/\text{Fe}_2\text{O}_3$ nanorods are found to be porous, which is attributed to high temperature dehydration process during the calcination treatment.

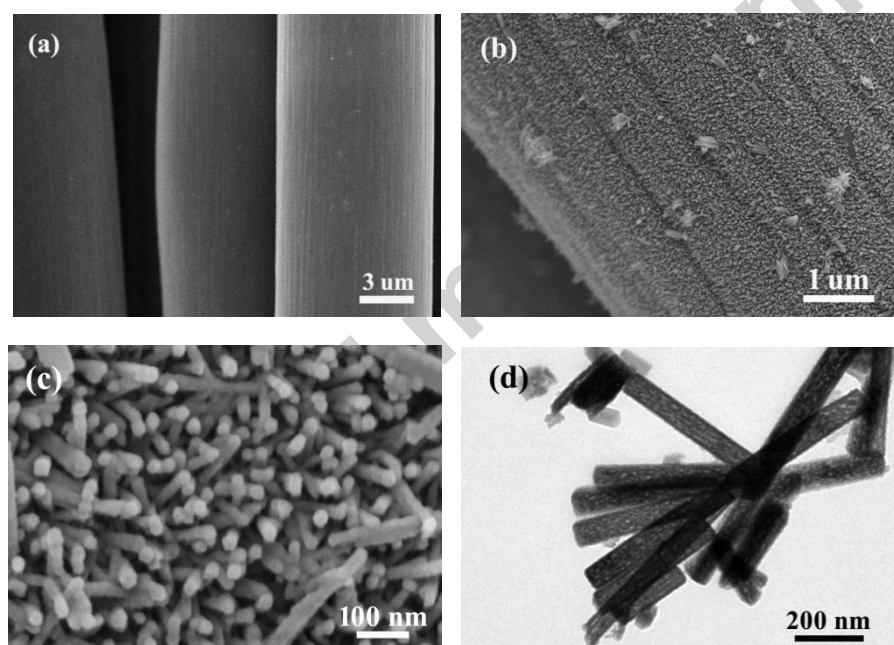


Fig. 2. SEM images of (a) blank carbon fiber cloth, (b, c) $\text{CoFe}_2\text{O}_4/\text{Fe}_2\text{O}_3$ nanorod arrays on carbon fiber cloth.
(d) TEM image of $\text{CoFe}_2\text{O}_4/\text{Fe}_2\text{O}_3$ nanorod arrays.

After UV- light irradiation process, Ag nanoparticles were loaded on the surface of $\text{CoFe}_2\text{O}_4/\text{Fe}_2\text{O}_3$ nanorod arrays. SEM was firstly used to investigate the morphology of the obtained $\text{Ag}@ \text{CoFe}_2\text{O}_4/\text{Fe}_2\text{O}_3$ nanorod arrays composite. Only nanorods can be clearly seen (Fig. S1). Fig. 3a shows TEM and HRTEM images of the obtained $\text{Ag}@ \text{CoFe}_2\text{O}_4/\text{Fe}_2\text{O}_3$ nanorod arrays. It can be seen

numerous Ag nanoparticles with sizes ranging from 10 to 40 nm are decorated on the $\text{CoFe}_2\text{O}_4/\text{Fe}_2\text{O}_3$ nanorod arrays. The Ag nanoparticles have high crystalline with clear lattice fringes, as verified by the HRTEM result (Fig.3(b)). The lattice fringes with spacing of 0.232 nm and 0.250 nm can be indexed into (111) plane of cubic Ag and (311) plane of CoFe_2O_4 , respectively. In order to investigate the distribution of related element in the sample, TEM elemental mapping was performed. The corresponding elemental maps (Fig. 3(c)) show the expected homogeneously spatial distribution of Co, Fe and O on the entire volume of the nanorods.

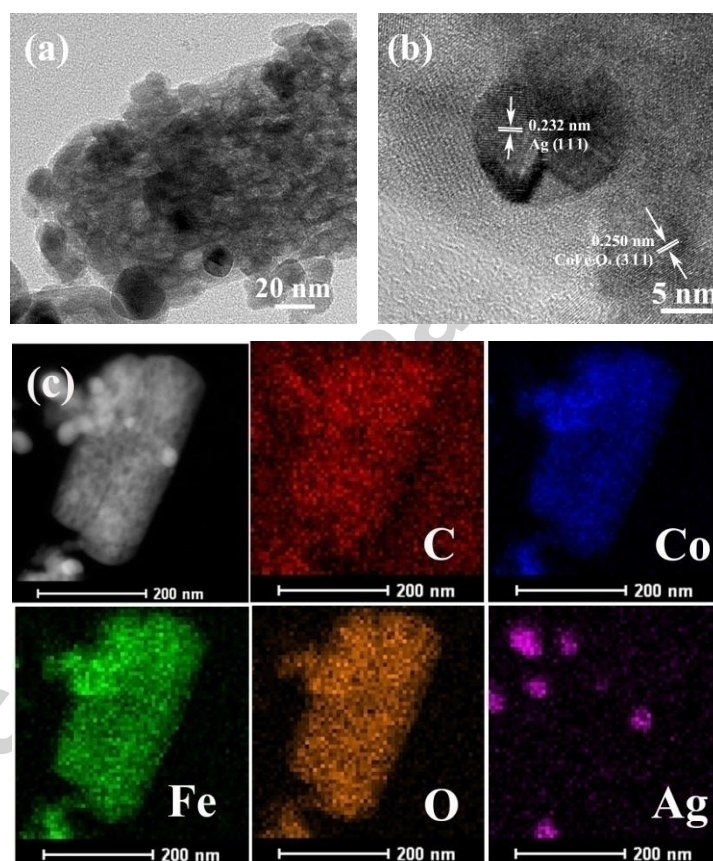


Fig. 3. (a) TEM image of $\text{Ag@CoFe}_2\text{O}_4/\text{Fe}_2\text{O}_3$ nanorods, (b) HRTEM image of a single Ag nanoparticle, (c) TEM mapping of C, Co, Fe, O, Ag on a nanorod.

To further study oxidation state and chemical composition of the $\text{Ag@CoFe}_2\text{O}_4/\text{Fe}_2\text{O}_3$ nanorod arrays product, XPS investigation was performed. As expected, Ag, O, Fe and Co elements can be seen in the

XPS full spectrum (Fig. 4(a)). As shown in the Fig. 4(b), there are two split peaks at 711.2 and 724.6 eV, which can be corresponded to Fe 2p_{3/2} and Fe 2p_{1/2}, respectively. Of the two peaks Fe 2p_{3/2} peak is narrower and stronger than Fe 2p_{1/2} and the area of Fe 2p_{3/2} peak is greater than that of Fe 2p_{1/2} because of spin-orbit (j-j) coupling. In addition, two satellite peaks located at 718.8 and 729.5 eV was also observed [35]. The result shows that Fe³⁺ exists in the Ag@CoFe₂O₄/Fe₂O₃ nanorod arrays sample. Two distinct peaks at 780.6 eV for Co 2p_{3/2} and 796.4 eV for Co 2p_{1/2} with shakeup satellite peaks at 787.4 and 803.9 eV are observed in Fig.4(c), which is characteristic of Co²⁺ in the composite [36]. Two peaks for Ag 3d are observed at 368.4 and 374.4 eV (Fig. 4(d)), assigned to Ag 3d_{5/2} and Ag 3d_{3/2}, respectively, which are the typical values for metallic Ag [37]. These results clearly proved the successfully fabrication of Ag nanoparticles loaded on the surface of CoFe₂O₄/Fe₂O₃ nanorod arrays.

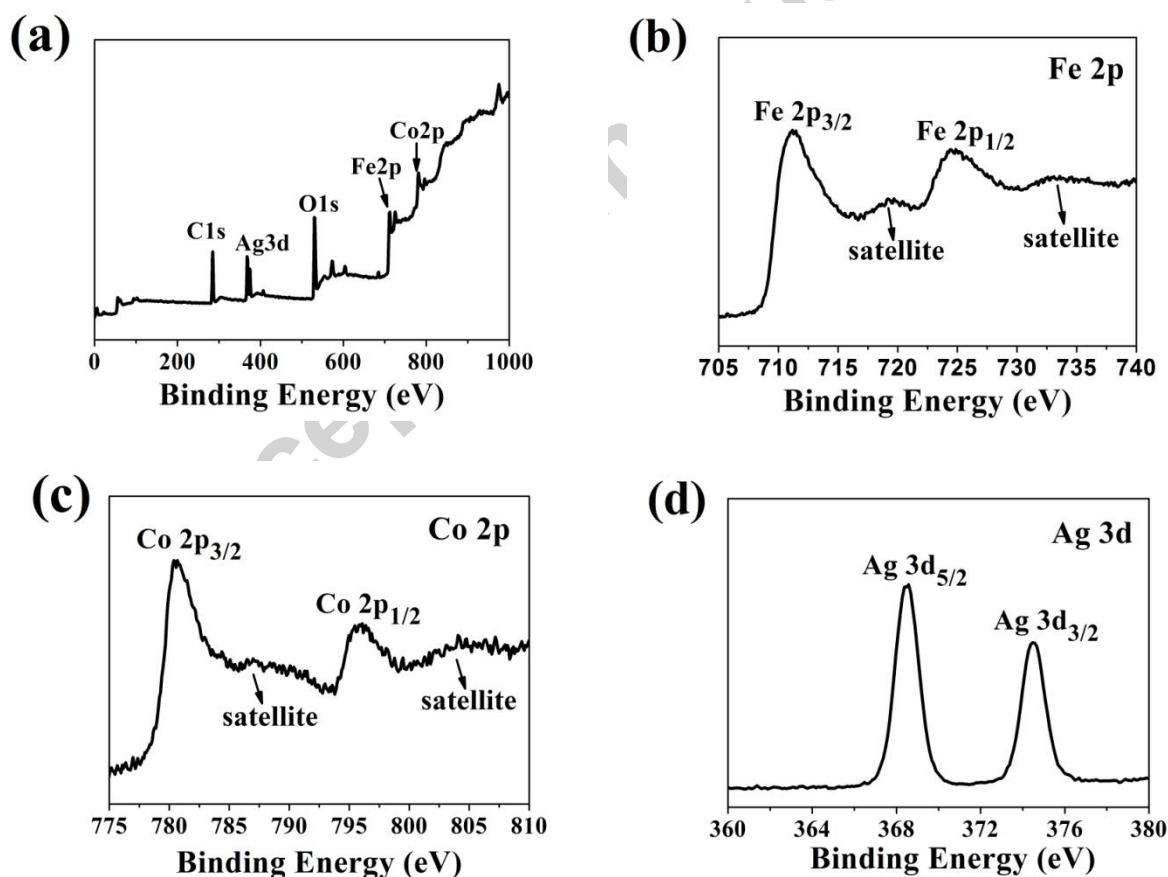


Fig.4. XPS spectra of the synthesized Ag@CoFe₂O₄/Fe₂O₃ nanorod arrays. (a) The whole XPS spectrum, (b) Fe2p XPS spectrum, (c) Co2p XPS spectrum, (d) Ag3d XPS spectrum.

It is well known that the surface plasmon resonance induced by noble metal nanoparticles can highly enhance the Raman signal of the adsorbed molecular. To investigate the SERS activity of the Ag@CoFe₂O₄/Fe₂O₃ nanorod arrays, R6G was chosen as the model molecule. The carbon fiber cloth loaded with Ag@CoFe₂O₄/Fe₂O₃ nanorod arrays was firstly soaked in 3 mL of R6G solution for 12 h before SERS investigation. Fig. 5(a) shows the SERS spectrum of 10⁻⁶ M R6G solution collected with Ag@CoFe₂O₄/Fe₂O₃ nanorod arrays substrate. For comparison, the SERS spectrum collected with 0.1 M R6G on pure carbon fiber cloth substrate is also shown in Fig. 5. It can be clearly seen that the SERS spectrum collected with Ag@CoFe₂O₄/Fe₂O₃ nanorod arrays substrate shows clear and much high Raman vibration features for R6G at 610, 772, 1183, 1310, 1361, 1505, 1573, and 1649 cm⁻¹, well consistent with previously reported data [8]. In contrast, very weak Raman peaks are shown with pure carbon fiber cloth substrate, although the R6G concentration is much higher (0.1 M).

In order to demonstrate SERS performance quantitatively, the enhancement factor (EF) was calculated based on the pure carbon fiber cloth substrate and 0.1 M R6G according to the following formula:

$$EF = \frac{I_{SERS} N_0}{I_0 N_{SERS}} = \frac{I_{SERS} n_0 N_A}{I_0 n_{SERS} N_A} = \frac{I_{SERS} C_0 V_0}{I_0 C_{SERS} V_{SERS}} = \frac{I_{SERS} C_0}{I_0 C_{SERS}}$$

N_0 is the molecule number of 0.1 M of R6G solution and I_0 is the corresponding intensity. N_{SERS} and I_{SERS} are those with our prepared SERS substrate measurement under the concentration of 10⁻⁶ M. All the Raman intensity and the calculation are based on the peak at 1649 cm⁻¹, and the value of the I_0 is 2031.3. According to this formula, the Ag@CoFe₂O₄/Fe₂O₃ nanorod arrays provide EF of about 6.1×10⁵ with I_{SERS} of 12302.0. For comparison, Ag nanoparticles loaded on the carbon fiber cloth was also prepared with the same photochemical method and used as SERS substrate. It's Raman intensity is 2091.6 at the peak of 1649 cm⁻¹, showing the EF of about 1.0 10⁵, which is lower than that of Ag@CoFe₂O₄/Fe₂O₃ nanorod arrays (Fig. S2). Another compared experiment shows that there is no R6G Raman signal detected by using CoFe₂O₄/Fe₂O₃ nanorod arrays as SERS substrate, which means the Raman signal enhancement is only due to the surface plasmon resonance of the Ag nanoparticles

(Fig. S3). It seems that there is a synergistic effect between $\text{CoFe}_2\text{O}_4/\text{Fe}_2\text{O}_3$ nanorod arrays and Ag, which induces the enhanced SERS performance. It is possible that the rod-like $\text{CoFe}_2\text{O}_4/\text{Fe}_2\text{O}_3$ nanorod arrays make the loaded Ag nanoparticles have more hot spots, and so higher EF factor.

To evaluate the detection sensitivity of the $\text{Ag}@\text{CoFe}_2\text{O}_4/\text{Fe}_2\text{O}_3$ nanorod arrays substrate, SERS spectra of the substrate immersed in different concentrations of R6G solution (10^{-8} , 10^{-9} and 10^{-10} M) were measured. As shown in Fig. 5(b), it can clearly distinguish the characteristic bands of 10^{-10} M of R6G. The values of the Raman intensity based on the peak at 1649 cm^{-1} for 10^{-8} M, 10^{-9} M and 10^{-10} M of R6G solution are 4708.3, 2434.4 and 206.5, respectively. And the corresponding EF values were calculated to be about 2.3×10^7 , 1.2×10^8 and 1.0×10^8 , respectively.

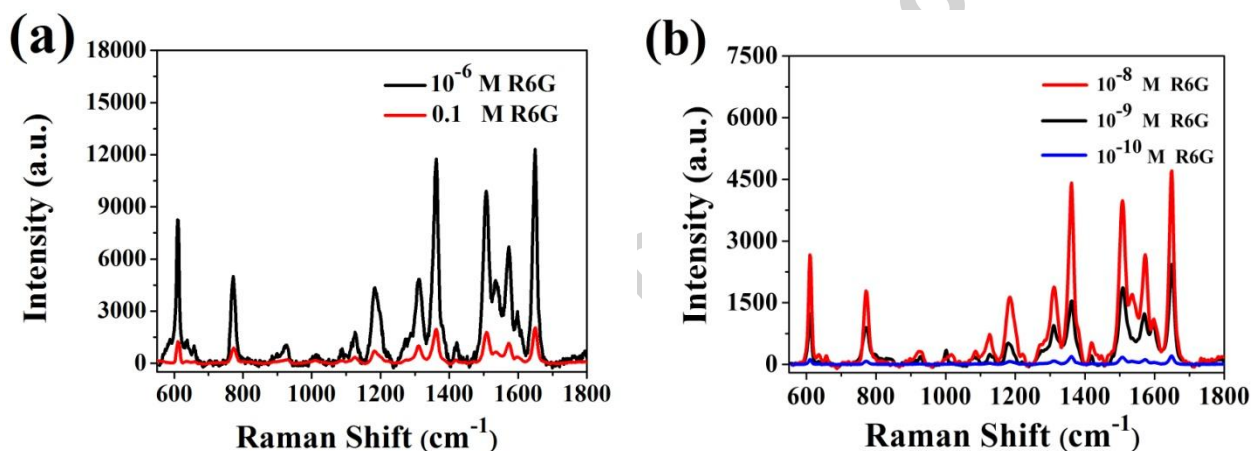


Fig. 5. (a) SERS spectra of 10^{-6} M R6G solution adsorbed on the $\text{Ag}@\text{CoFe}_2\text{O}_4/\text{Fe}_2\text{O}_3$ nanorod arrays substrate and 0.1 M R6G adsorbed on pure carbon fiber cloth substrate. (b) Raman scattering spectra of the $\text{Ag}@\text{CoFe}_2\text{O}_4/\text{Fe}_2\text{O}_3$ nanorod arrays substrate immersed in R6G aqueous solutions with concentration of 10^{-8} M, 10^{-9} M and 10^{-10} M.

The stability and uniformity is quite important for a SERS substrate [38-39]. To further test the stability and uniformity of the $\text{Ag}@\text{CoFe}_2\text{O}_4/\text{Fe}_2\text{O}_3$ nanorod arrays substrate, the Raman mapping was scanned over a $20 \times 20\ \mu\text{m}^2$ area with a step size of $2\ \mu\text{m}$. 100 points were collected. The SERS mapping of 10^{-6} M R6G solution on the $\text{Ag}@\text{CoFe}_2\text{O}_4/\text{Fe}_2\text{O}_3$ nanorod arrays substrate was shown in Fig.6(a). The relative standard deviations (RSD) of Raman peaks at 1311 , 1508 , and 1649 cm^{-1} on the mapping was calculated to be 11.99%, 11.76%, and 11.85%, respectively (Fig.6(b-e)), indicating a

good Raman signal reproducibility of the as-prepared Ag@CoFe₂O₄/Fe₂O₃ nanorod arrays substrate. It is believed that CoFe₂O₄/Fe₂O₃ nanorod arrays with high uniformity may contribute to a 3D ordered arrangement of Ag nanoparticles. So many 3D hot spots would be formed between adjacent nanorods, which induce higher EF values and good Raman signal reproducibility.

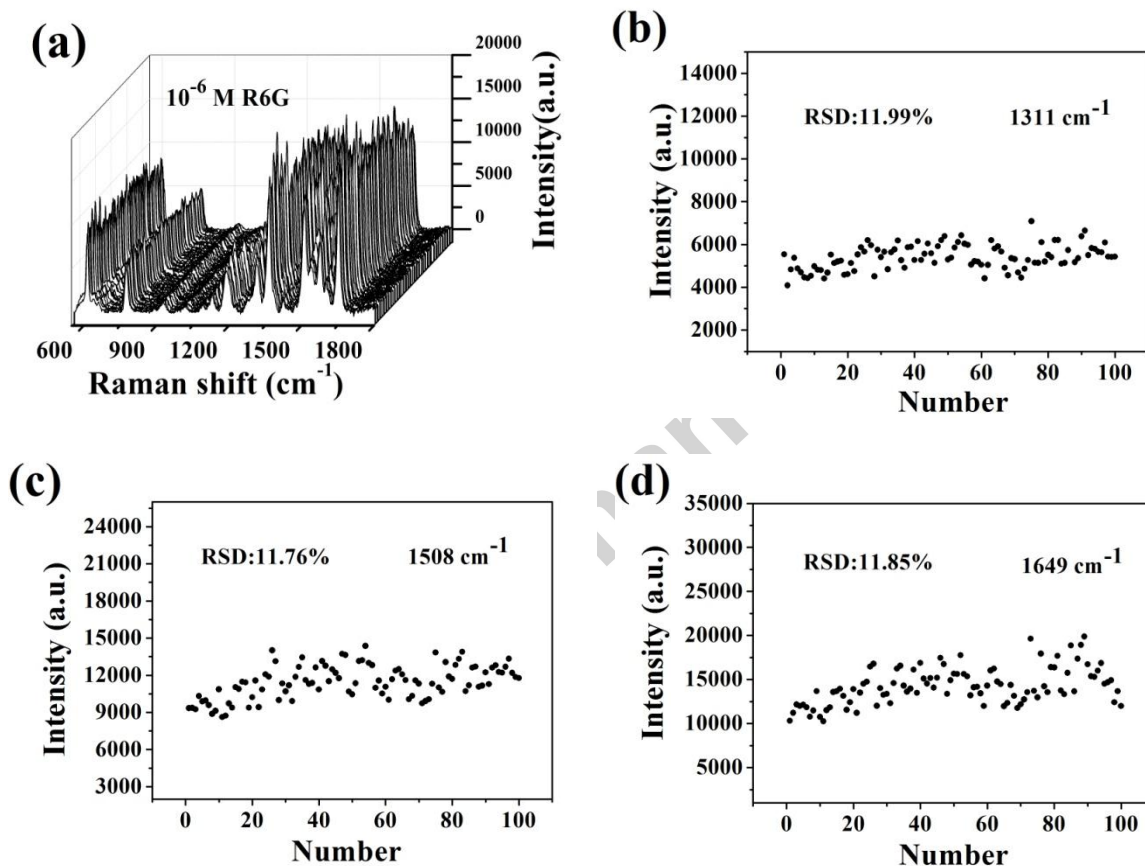


Fig.6. (a) Raman scattering spectra of 10⁻⁶ M R6G measured by 100 points over a 20 × 20 μm² area with a step size of 2 μm. (b-d) The main Raman vibration intensities of R6G in SERS spectra showed in (a).

As for an effective SERS substrate that can be repeatedly used for many times, removing of the surface absorbed molecules is necessary. However, due to the high sensitivity of SERS, direct cleaning of the surface absorbed molecules to be no Raman signal state is quite difficult. Our prepared Ag@CoFe₂O₄/Fe₂O₃ nanorod-based SERS substrate would be cleaned with photocatalytic mechanism, since the Ag@CoFe₂O₄/Fe₂O₃ nanorod arrays also shows photocatalytic activity.

Photo-Fenton activity of the Ag@CoFe₂O₄/Fe₂O₃ nanorod arrays was then investigated by monitoring the degradation of R6G (5 mg/L) under visible light irradiation. The photocatalytic activity was measured by recording the UV-vis spectra of the R6G solution after different irradiation times. As shown in Fig.7(a), with the increase of photocatalytic degradation time, the absorption band intensity of R6G at 526 nm significantly decreases, indicating the gradual breakdown of the chromophore structure responsible for the color of the dye. The percentage of the R6G degraded can be calculated using the following equation [40]:

$$\% \text{ degradation} = \frac{C_0 - C_t}{C_0} \times 100$$

Where C_0 is the initial R6G concentration and C_t is the concentration at time t . According to the equation, under the visible light irradiation, 99.15% of R6G could be degraded over the Ag@CoFe₂O₄/Fe₂O₃ nanorod arrays after 1 h. In contrast, CoFe₂O₄/Fe₂O₃ nanorod arrays without Ag nanoparticles loading only show degradation of 51.5%. For comparison, photocatalytic degradation of R6G in absence of the catalyst was also performed (Fig. 7(b)), only 22.4% of R6G were degraded. In addition, without the catalyst and H₂O₂, only 0.64% of R6G were degraded.

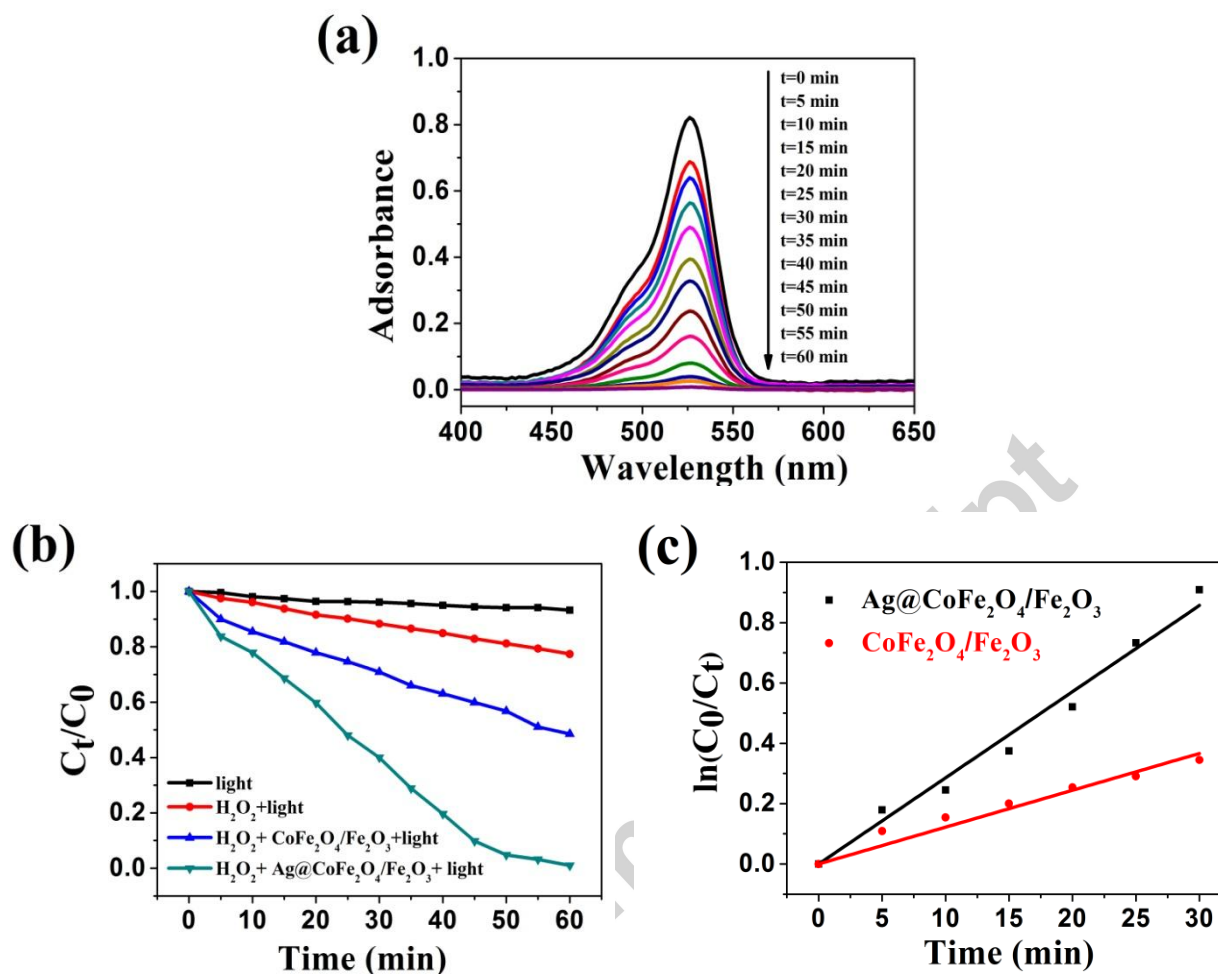


Fig. 7. (a) Time-dependent UV-vis absorption spectra of R6G solution in the present of a piece of Ag@CoFe₂O₄/Fe₂O₃ nanorod arrays. (b) The degradation rate curve of R6G in different conditions. (c) Photodegradation kinetics of R6G in the presence of Ag@CoFe₂O₄/Fe₂O₃ nanorod arrays and CoFe₂O₄/Fe₂O₃ nanorod arrays.

The kinetics of photocatalytic degradation of R6G in the presence of Ag@CoFe₂O₄/Fe₂O₃ nanorod arrays and CoFe₂O₄/Fe₂O₃ nanorod arrays were further investigated. In terms of the modified Langmuir-Hinshelwood (L-H) model [40, 41], the kinetic equation could be expressed as:

$$r = -\frac{dC}{dt} = \frac{k_r K_{LH} C}{1 + K_{LH} C} = kC$$

Where r ($\text{mg L}^{-1} \text{min}^{-1}$) is the reaction rate, C (mg L^{-1}) is the reactant concentration, t (min) is the time

of irradiation, k_r ($\text{mg L}^{-1} \text{min}^{-1}$) is the reaction rate constant K_{LH} (L mg^{-1}) is the adsorption constant, and k (min^{-1}) is the pseudo first order rate constant. By integrating at the limit of $C=C_0$ at $t=0$, the above formula can be expressed as:

$$\ln \frac{C_0}{C} = kt$$

The plots of $\ln (C_0/C)$ versus t for the two catalysts are shown in Fig. 7(c). The rate constant of the reaction with the catalyst of Ag@CoFe₂O₄/Fe₂O₃ nanorod arrays is 0.02856 min^{-1} , which is much higher than that of CoFe₂O₄/Fe₂O₃ nanorod arrays (0.01222 min^{-1}). This means that the existence of Ag nanoparticles is beneficial for the photo-Fenton reaction.

A possible mechanism to the enhanced photocatalytic performance of Ag nanoparticles loaded CoFe₂O₄/Fe₂O₃ nanorod arrays can be put forward. Firstly, the ferrite was irradiated by the light. An electron/hole (e^-/h^+) pair was generated on the surface. The photogenerated hole h_{VB}^+ could react with water or a hydroxyl ion (H_2O or OH^-) to generate a hydroxyl radical, while the photogenerated electron e_{CB}^- could be captured by H_2O_2 to yield hydroxyl radicals, limiting the recombination of holes and electrons, thus improving the photocatalytic activity. With Ag nanoparticles loading, the excited electrons in the conduction band of ferrite would be trapped by Ag species, which is favorable for the separation of photo-generated electrons and holes [42, 43]. This will subsequently help to form active radicals to degrade the adsorbed pollutants.

Considering the high photocatalytic activity, the recycling of the Ag@CoFe₂O₄/Fe₂O₃ nanorod arrays SERS substrate was then tested. The used Ag@CoFe₂O₄/Fe₂O₃ SERS substrate was cleaned with H_2O_2 solution with the assistance of light irradiation. After the cleaning process, it was reused as SERS substrate. The Raman signal collected on this reused substrate is shown in Fig. 8. It can be seen that R6G Raman signals still can be clearly seen after the fifth cycle. The Raman intensity values of five cycles based on the peak at 1649 cm^{-1} are 12302.0, 2479.2, 1418.5, 1021.6 and 405.1, respectively. The EF values were calculated to be about 6.1×10^5 , 1.2×10^5 , 7.0×10^4 , 5.0×10^4 and 2.0×10^4 , respectively. The decrease of the EF value would be partially due to the loss of Ag nanoparticles during the treatment process. This result suggests that the obtained Ag@CoFe₂O₄/Fe₂O₃ nanorod

arrays substrates can act both as SERS substrate and as photocatalysts. This bifunctions facilitates the recycling of the SERS substrates.

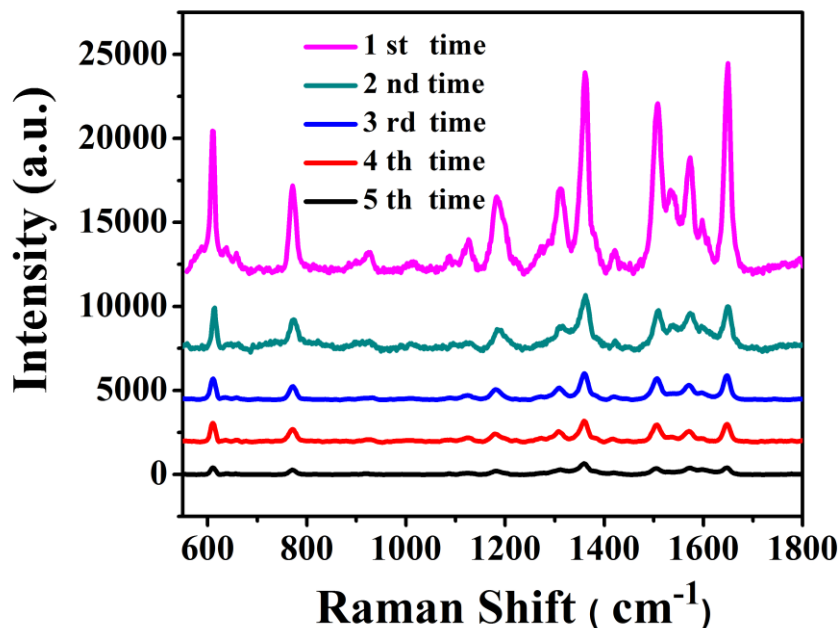


Fig. 8. Recycling of the Ag@CoFe₂O₄/Fe₂O₃ nanorod arrays SERS substrate. SERS spectra of 10⁻⁶ M R6G solution with a piece of used Ag@CoFe₂O₄/Fe₂O₃ nanorod arrays.

4. Conclusions

In summary, CoFe₂O₄/Fe₂O₃ nanorod arrays on carbon fiber cloth have been successfully synthesized through a simple hydrothermal synthesis method followed by calcining treatment. Ag nanoparticles were decorated on the CoFe₂O₄/Fe₂O₃ nanorod arrays by the following photochemical process to form Ag@CoFe₂O₄/Fe₂O₃ nanorod arrays composite. The obtained composite can be used as SERS substrate with high EF value and high reproducibility with RSD value less than 12%. In addition, the composite can be used as effective photo-Fenton catalyst to degrade R6G solution. Due to the bifunctions, the recycling of the Ag@CoFe₂O₄/Fe₂O₃ nanorod arrays composite as SERS substrate was demonstrated.

Acknowledgements

The authors are grateful for support of Jiangsu Overseas Research & Training Program for University Prominent Young & Middle-aged Teachers and Presidents, Jiangsu Government Scholarship for Overseas Study & Jiangsu University Scholarship for Overseas Study, National Natural Science Foundation of China (No.21776115), Natural Science Foundation of Jiangsu province (No. BK20161343), Qing Lan Project of Jiangsu Province, the project of the Priority Academic Program Development of Jiangsu Higher Education Institutions.

Conflict of interest

The authors declare that they have no conflict of interest.

References

- [1] J. F. Li, Y. J. Zhang, S. Y. Ding, R. Panneerselvam, Z. Q. Tian, Core-shell nanoparticle-enhanced Raman spectroscopy, *Chem. Rev.* 117 (2017) 5002-5069.
- [2] I. Alessandri, J. R. Lombardi, Enhanced Raman scattering with dielectrics, *Chem. Rev.* 116 (2016) 14921-14981.
- [3] S. Schlücker, Surface-enhanced Raman spectroscopy: concepts and chemical applications, *Angew. Chem. Int. Ed.* 53 (2014) 4756-4795.
- [4] S. L. Kleinman, R. R. Frontiera, A. I. Henry, J. A. Dieringer, R. P. Van Duyne, Creating, characterizing, and controlling chemistry with SERS hot spots, *Phys. Chem. Chem. Phys.* 15 (2013) 21-36.
- [5] H. Ko, S. Singamaneni, V. V. Tsukruk, Nanostructured surfaces and assemblies as SERS media, *Small* 4 (2008) 1576-1599.
- [6] S. M. Nie, S. R. Emery, Probing single molecules and single nanoparticles by surface-enhanced Raman scattering, *Science* 275 (1997) 1102-1106.

- [7] B. N. Khlebtsov, Z. Liu, J. Ye, N. G. Khlebtsov, Au@Ag core/shell cuboids and dumbbells: optical properties and SERS response, *J. Quant. Spectrosc. Radiat. Transfer* 167 (2015) 64-75.
- [8] Y. L. Shen, Y. J. Liu, W. Wang, F. Xu, C. Yan, A. H. Yuan, Au nanocluster arrays on self-assembled block copolymer thin films as highly active SERS substrates with excellent reproducibility, *RSC Adv.* 6 (2016) 38716-38723.
- [9] A. E. Rider, S. Kumar, S. A. Furman, K. Ostrikov, Self-organized Au nanoarrays on vertical graphenes: an advanced three-dimensional sensing platform, *Chem. Commun.* 48 (2012) 2659-2661.
- [10] X. L. Zhang, X. H. Xiao, Z. G. Dai, W. Wu, X.G. Zhang, L. Fu, C. Z. Jiang, Ultrasensitive SERS performance in 3D "sunflower-like" nanoarrays decorated with Ag nanoparticles, *Nanoscale* 9 (2017) 3114-3120.
- [11] G. Barbillon, V. E. Sandana, C. Humbert, B. Belier, D. J. Rogers, F. H. Teherani, P. Bove, R. McClintock, M. Razeghi, Study of Au coated ZnO nanoarrays for surface enhanced Raman scattering chemical sensing, *J. Mater. Chem. C* 5 (2017) 3528-3525.
- [12] S. G. Park, T. Y. Jeon, H. C. Jeon, J. D. Kwon, C. W. Mun, M. K. Lee, B. Cho, C. S. Kim, M. Song, D. H. Kim, Fabrication of Au-decorated 3D ZnO nanostructures as recyclable SERS substrates, *IEEE. Sens. J* 16 (2016) 3382-3386.
- [13] Z. Y. Bao, X. Liu, J. Dai, Y. Wu, Y. H. Tsang, D. Lei, In situ SERS monitoring of photocatalytic organic decomposition using recyclable TiO₂-coated Ag nanowire arrays, *Appl. Surf. Sci.* 301 (2014) 351-357.
- [14] A. Lamberti, A. Virga, A. Chiadò, A. Chiodoni, K. Bejtka, P. Rivolo, F. Giorgis, Ultrasensitive Ag-coated TiO₂ nanotube array for flexible SERS-based optofluidic devices, *J. Mater. Chem. C* 3 (2015) 6868-6875.
- [15] Q. Zhou, G. Meng, Q. Huang, C. Zhu, H. Tang, Y. Qian, B. Chen, B. Chen, Ag-nanoparticles-decorated NiO-nanoflakes grafted Ni-nanorod arrays stuck out of porous AAO as effective SERS substrates, *Phys. Chem. Chem. Phys.* 16 (2014) 3686-3692.
- [16] H. L. Liu, Z. L. Yang, L. Y. Meng, Y. D. Sun, J. Wang, L. B. Yang, J. H. Liu, Z. Q. Tian, Three-dimensional and time-ordered surface-enhanced Raman scattering hotspot matrix, *J. Am. Chem.*

Soc. 136 (2014), 5332-5341.

[17] A. S. Urban, X. S. Sun, Y. M. Wang, N. Large, H. Wang, M. W. Knight, P. Nordlander, H. Y. Chen, N. J. Halas, Three-dimensional plasmonic nanoclusters, *Nano Lett.* 13 (2013) 4399-4403.

[18] A. Martín, A. Pescaglini, C. Schopf, V. Scardaci, R. Coull, L. Byrne, D. Iacopino, Surface-enhanced Raman scattering of 4-aminobenzenethiol on Au nanorod ordered arrays, *J. Phys. Chem. C* 118 (2014) 13260-13267.

[19] H. Im, K. C. Bantz, S. H. Lee, T. W. Johnson, C. L. Haynes, S. H. Oh, Self-assembled plasmonic nanoring cavity arrays for SERS and LSPR biosensing, *Adv. Mater.* 25 (2013) 2678-2685.

[20] Z. Zhang, Y. Z. Jiang, M. Q. Chi, Z. Z. Yang, G. D. Nie, X. F. Lu, C. Wang, Fabrication of Au nanoparticles supported on CoFe₂O₄ nanotubes by polyaniline assisted self-assembly strategy and their magnetically recoverable catalytic properties, *Appl. Surf. Sci.* 363 (2016) 578-585.

[21] L. L. Zhang, Z. W. Bao, X. X. Yu, P. Dai, J. Zhu, M. Z. Wu, G. Li, X. S. Liu, Z. Q. Sun, C. L. Chen, Rational design of α -Fe₂O₃/reduced graphene oxide composites: rapid detection and effective removal of organic pollutants, *ACS Appl. Mater. Interf.* 8 (2016) 6431-6438.

[22] S. Adhikari, D. Sarkar, G. Madras, Hierarchical design of CuS architectures for visible light photocatalysis of 4-chlorophenol, *ACS Omega* 2 (2017) 4009-4021.

[23] Q. Cao, X. Liu, K. P. Yuan, J. Yu, Q. H. Liu, J. J. Delaunay, R. C. Che, Gold nanoparticles decorated Ag(Cl, Br) micro-necklaces for efficient and stable SERS detection and visible-light photocatalytic degradation of Sudan I, *Appl. Catal. B-Environ.* 201 (2017) 607-616.

[24] C. Y. Wen, F. Liao, S. S. Liu, Y. Zhao, Z. H. Kang, X. L. Zhang, M. W. Shao, Bi-functional ZnO-RGO-Au substrate: photocatalysts for degrading pollutants and SERS substrates for real-time monitoring, *Chem. Commun.* 49 (2013) 3049-3051.

[25] Y. Zhao, L. Sun, M. Xi, Q. Feng, C. Y. Jiang, H. Fong, Electrospun TiO₂ nanofelt surface-decorated with Ag nanoparticles as sensitive and UV-cleanable substrate for surface enhanced Raman scattering, *ACS Appl. Mater. Interf.* 6 (2014) 5759-5767.

- [26] X. Li, G. Chen, L. Yang, Z. Jin, J. Liu, Multifunctional Au-coated TiO₂ nanotube arrays as recyclable SERS substrates for multifold organic pollutants detection. *Adv. Funct. Mater.* 20 (2010) 2815-2824.
- [27] Z. Y. Bao, X. Liu, J. Y. Dai, Y. C. Wu, Y. H. Tsang, D. Y. Lei, In situ SERS monitoring of photocatalytic organic decomposition using recyclable TiO₂-coated Ag nanowire arrays, *Appl. Surf. Sci.* 301 (2014) 351-357.
- [28] Y. S. Zang, J. Yin, X. He, C. Yue, Z. M. Wu, J. Li, J. Y. Kang, Plasmonic-enhanced self-cleaning activity on asymmetric Ag/ZnO surface-enhanced Raman scattering substrates under UV and visible light irradiation, *J. Mater. Chem. A* 2 (2014) 7747-7753.
- [29] E. Casbeer, V. K. Sharma, X. Z. Li, Synthesis and photocatalytic activity of ferrites under visible light: a review, *Sep. Purif. Technol.* 87 (2012) 1-14.
- [30] Y. Zhou, B. Xiao, S. Q. Liu, Z. D. Meng, Z. G. Chen, C. Y. Zou, C. B. Liu, F. Chen, X. Zhou, Photo-Fenton degradation of ammonia via a manganese-iron double-active component catalyst of graphene-manganese ferrite under visible light, *Chem. Eng. J.* 283 (2016) 266-275.
- [31] Y. Ahmed, Z. Yaakob, P. Akhtar, Degradation and mineralization of methylene blue using a heterogeneous photo-Fenton catalyst under visible and solar light irradiation, *Catal. Sci. Technol.* 6 (2016) 1222-1232.
- [32] J. Deng, Y. S. Shao, N. Y. Gao, C. Q. Tan, S. Q. Zhou, X. H. Hu, CoFe₂O₄ magnetic nanoparticles as a highly active heterogeneous catalyst of oxone for the degradation of diclofenac in water, *J. Hazard. Mater.* 262 (2013) 836-844.
- [33] S. Q. Liu, L. R. Feng, N. Xu, Z. G. Chen, X. M. Wang, Magnetic nickel ferrite as a heterogeneous photo-Fenton catalyst for the degradation of rhodamine B in the presence of oxalic acid, *Chem. Eng. J.* 203 (2012) 432-439.
- [34] S. Jauhar, S. Singhal, M. Dhiman, Manganese substituted cobalt ferrites as efficient catalysts for H₂O₂, assisted degradation of cationic and anionic dyes: their synthesis and characterization, *Appl. Catal. A- Gen.* 486 (2014) 210-218.

- [35] T. Yamashita, P. Hayes, Analysis of XPS spectra of Fe^{2+} and Fe^{3+} ions in oxide materials, *Appl. Surf. Sci.* 254 (2008) 2441-2449.
- [36] S. Lee, J. S. Kang, K. T. Leung, W. Lee, D. Kim, S. Han, W. Yoo, H. J. Yoon, K. Nam, Y. Sohn, Unique multi-phase $\text{Co/Fe/CoFe}_2\text{O}_4$ by water-gas shift reaction, CO oxidation and enhanced supercapacitor performances, *J. Ind. Eng. Chem.* 43(2016) 69-77.
- [37] G. B. Hoflund, Z. F. Hazos, G. N. Salaita, Surface characterization study of Ag, AgO, and Ag_2O using x-ray photoelectron spectroscopy and electron energy-loss spectroscopy, *Phy. Rev. B* 62 (2000) 11126-11133.
- [38] Q. Fu, Z. Zhan, J. Dou, X. Z. Zheng, R. Xu, M. H. Wu, Y. Lei, Highly reproducible and sensitive SERS substrates with Ag inter-nanoparticle gaps of 5-nm fabricated by ultrathin aluminum mask technique, *ACS Appl. Mater. Interf.* 7 (2015) 13322-13328.
- [39] J. Zhou, F. Zhu, Y. Wang, T. Wang, One-step green synthesis of high uniform SERS substrate based on Au nanoparticles grown on Ge wafer, *Chem. Phys. Lett.* 627 (2015) 96-100.
- [40] R. Sharm, S. Bansal, S. Singhal, Tailoring the photo-Fenton activity of spinel ferrites (MFe_2O_4) by incorporating different cations (M= Cu, Zn, Ni and Co) in the structure, *RSC. Adv.* 5 (2015) 6006-6018.
- [41] T. Soltani, M. H. Entezari, Photolysis and photocatalysis of methylene blue by ferrite bismuth nanoparticles under sunlight irradiation, *J. Mol. Catal. A: Chem.* 377 (2013) 197-203.
- [42] Y. Tian, T. Tatsuma, Mechanisms and applications of plasmon-induced charge separation at TiO_2 films loaded with gold nanoparticles, *J. Am. Chem. Soc.* 127 (2005) 7632-7637.
- [43] Z. R. Zhu, X. Y. Li, Q. D. Zhao, H. Li, Y. Shen, G.H. Chen, Porous "brick-like" NiFe_2O_4 nanocrystals loaded with Ag species towards effective degradation of toluene, *Chem. Eng. J.* 165 (2010) 64-70.